Quantitative Comparison of the Hydrogen Bond Network of A-State and Native Ubiquitin by Hydrogen Bond Scalar Couplings†

Florence Cordier* and Stephan Grzesiek*

Division of Structural Biology, Biozentrum der Universität Basel, 4056 Basel, Switzerland

Received April 7, 2004; Revised Manuscript Received June 30, 2004

ABSTRACT: The backbone hydrogen bond (H-bond) network of the partially folded A-state of ubiquitin (60% methanol, 40% water, pH 2) has been characterized quantitatively by $^{h3}J_{NC'}$ H-bond scalar couplings between the ^{15}N nuclei of amino acid H-bond donors and the ^{13}C carbonyl nuclei of the acceptors. Results on $^{h3}J_{NC'}$ couplings and the amide proton ($^1H^N$) chemical shifts for the A-state are compared quantitatively to the native state. The $^{h3}J_{NC'}$ correlations of the A-state show intact, nativelike H-bonds of the first β-hairpin $\beta1/\beta2$ and the α-helix, albeit at lower strength, whereas the H-bonds in the C-terminal part change from a pure β-structure to an all α-helical $H^N(i)\rightarrow O(i-4)$ connectivity pattern. A residue-specific analysis reveals that the conformations within the conserved secondary structure segments are much more homogeneous in the A-state than in the native state. Thus, the strong asymmetry of $^{h3}J_{NC'}$ couplings and $^1H^N$ chemical shifts between the interior and exterior sides of the native state α-helix vanishes in the A-state. This indicates that the bend of this helix around the native state hydrophobic core is released in the homogeneous solvent environment of the A-state. Similarly, an irregularity in the behavior of H-bond I3→L15 in hairpin $\beta1/\beta2$, which results from strong contacts to strand $\beta5$ in the native state, is absent in the A-state. These findings rationalize the behavior of the $^1H^N$ chemical shifts in both states and indicate that the A-state is in many aspects similar to the onset of thermal denaturation of the native state.

Many proteins adopt partially folded states under certain non-native conditions such as extremely low or high pH, high salt concentration, high temperature or by the addition of denaturants or organic solvents. These dynamic structures are usually characterized by an intermediate volume between the native and a completely unfolded state, the presence of a significant fraction of nativelike secondary structure, high flexibility, and the lack of stable tertiary contacts (*1*−*4*). Besides a general interest in the understanding of interactions responsible for protein stabilization, the research of partially folded states is motivated by the finding that certain of these destabilized structures represent equilibrium analogues of kinetic folding intermediates (*2*, *5*). Therefore, their characterization may also give insights into natural protein folding pathways.

A partially structured, stable state of the protein ubiquitin exists at room temperature in a 60%/40% methanol/water mixture at pH 2 (*6*). This so-called A-state has been intensively characterized by a variety of methods such as circular dichroism (CD) (*6*, *7*), hydrogen exchange (*8*, *9*), NMR (*10*−*12*), calorimetry (*13*), and molecular dynamics simulations (*14*, *15*).

The characterization by CD (*6*) and NMR (*11*, *12*) of the A-state has converged to the following conclusions about its residual average structure (see also Figure 1). A stable hydrophobic core is absent, and the overall shape is less globular than the native state. Nevertheless, certain secondary elements can be clearly detected. In the N-terminal part, the first antiparallel β-hairpin $\beta1/\beta2$ (residues M1 to V17) and the central α-helix α (residues I23 to G35) of the native state preserve their secondary conformation in the A-state. The C-terminal part beyond residue 35 undergoes a dramatic change from an all β-structure in the native state to a helical structure for residues Q40−R74 (helix α′) in the A-state. The structural conservation of the antiparallel β-hairpin $\beta1/\beta2$ and of helix α under changed solvent conditions suggests that the folding of these secondary structure elements may be independent from the rest of the protein. In fact, a peptide consisting of only the first 17 residues adopts a similar β-hairpin structure as this part of the entire protein in the A-state (*16*), and a peptide comprising the first 35 residues forms a structure that is similar to the β-hairpin and the central α-helix of the A-state (*7*).

The dynamical behavior of the A-state has been characterized by ^{15}N-relaxation data acquired at multiple magnetic fields (*12*). An interpretation of these data on a residue-by-residue basis using a generalized model-free approach indicates that the effective rotational correlation times are very different for the different protein segments. The shortest correlation times (4.5−6.5 ns) are found in the sheet and the longest ones (12−14 ns) in the C-terminal helix. This differential behavior and the particularly low $\{^1H\}-^{15}N$ NOE values around residues S20 and G35 suggest that the different segments are connected by flexible linkers. The N−H order parameters S^2 for most amino acids in all three segments have values (∼0.4−0.6) that are substantially lower than in folded globular proteins, and significant amounts of internal

† This work was supported by SNF Grant 3100-061757.00.

* To whom correspondence should be addressed. F.C.: phone, ++41 61 267 2080; fax, ++41 61 267 2109; e-mail, Florence.Cordier@unibas.ch. S.G.: phone, ++41 61 267 2100; fax, ++41 61 267 2109; e-mail, Stephan.Grzesiek@unibas.ch.

10.1021/bi049314f CCC: $27.50
Published on Web 08/14/2004

motion are detected for these residues on the nanosecond time scale. These results are partially reproduced by molecular dynamics simulations of the A-state (*14*, *15*), which show the loosely coupled nativelike secondary elements of the N-terminal part and the disappearance of the native structure in the C-terminal part.

Scalar couplings across hydrogen bonds (H-bonds) make it possible to directly observe the H-bond networks of biomacromolecules in COSY experiments (*17*). In the backbone of smaller proteins, the canonical N−H···O═C H-bond can be usually detected via H-bond $^{h3}J_{NC'}$ scalar couplings that connect the ^{15}N nucleus of the amino acid donor to the carbonyl ^{13}C nucleus of the acceptor (*18*, *19*). By their dependence on the overlap between hydrogen and acceptor orbitals (*20*, *21*), which results in a strong dependence on H-bond distances and angles (*18*, *21*−*24*), the couplings provide a very sensitive measure for the structure and dynamics of H-bonds and their changes under different conditions (*25*). In the present investigation, we have characterized the H-bond network of ubiquitin's A-state by $^{h3}J_{NC'}$ scalar couplings in an effort to understand the forces contributing to its stability. These data are compared quantitatively with ubiquitin's native state. Consistent with the earlier findings, the $^{h3}J_{NC'}$ correlations of the A-state show intact H-bonds of the first β-hairpin $\beta1/\beta2$ and the α-helix, albeit at lower strength, whereas the H-bonds in the C-terminal part change to an α-helical $H^N(i)\rightarrow O(i\text{-}4)$ connectivity pattern. A residue-specific analysis of the couplings and the $^1H^N$ chemical shift reveals that the H-bond conformations within the conserved secondary structure segments are much more homogeneous in the A-state than in the native state.

MATERIALS AND METHODS

Sample Preparation. Preparation of uniformly $^2H/^{15}N/^{13}C$-labeled ubiquitin with deuteration levels larger than 85% was performed as described previously (*26*). An NMR sample of 0.7 mM A-state ubiquitin was prepared by lyophilizing 350 μL of 1 mM triply labeled protein stock solution, pH 7, and dissolving it into 500 μL of a 40%/60% H_2O/CD_3OH (Cambridge Isotope Laboratories) mixture. The pH was then adjusted to 2. Note that a 0.7 mM concentration of A-state ubiquitin represents the upper limit for long-term sample stability, since higher concentrations lead to gelation after several weeks (*12*).

NMR Experiments. All NMR experiments were carried out at 25 °C on Bruker DRX600 or DRX800 spectrometers equipped with triple resonance pulse field gradient probeheads. The spectrometers were locked on the CD_3OH signal. Since the methanol hydroxyl protons resonate at a frequency very close to the water protons, solvent suppression was easily achieved by the normal WATERGATE (*27*) and water flip-back (*28*) schemes.

$^{h3}J_{NC'}$ Trans Hydrogen Bond Scalar Couplings. The $^{h3}J_{NC'}$ trans hydrogen bond scalar couplings were determined in the A-state of ubiquitin as described previously by long-range water flip-back 3D-HNCO experiments using TROSY detection of the slowly relaxing components of the $^1H-^{15}N$ doublet (*29*). Two sets of cross and reference 3D spectra were recorded at 800 MHz ^1H frequency as data matrices of $83^*(t_{CO}) \times 1024^*(t_{HN}) \times 28^*(t_N)$ data points (n^* is the number of complex points) with acquisition times of 39 ms (t_{CO}), 110 ms (t_{HN}), and 25 ms (t_N). The experimental times for cross and reference experiments were 31 h. The $^{h3}J_{NC'}$ couplings were calculated from the intensity ratio of the hydrogen bond cross-peaks (H_{Ni}, C'_j, N_i) to the reference peaks (H_{Ni}, C'_{i-1}, N_i) (*18*). To evaluate the reproducibility, a set of six 2D long-range H(N)CO experiments was also recorded at 600 MHz ^1H frequency with the same acquisition parameters (measuring time 22 h per experiment). The reported values for $^{h3}J_{NC'}$ couplings and their errors refer to means and standard deviations derived from these independent determinations. As judged by these standard deviations, a very high reproducibility of the scalar coupling values (on average better than 0.015 Hz) was achieved. $^{h3}J_{NC'}$ couplings of the native ubiquitin were taken from a previous study at 25 °C, pH 6.5 (*25*).

Other NMR Parameters. $^{13}C^\alpha$, $^{13}C^\beta$, and $^{13}C'$ chemical shift assignments were obtained from regular HNCA, HNCACB, and HNCO experiments. $^1H^N-^1H^N$ NOEs were determined from a 3D ^{15}N-edited NOESY with a mixing time of 360 ms.

RESULTS

Comparison of the H-Bond Network in the A-State and in the Native State. The transition from the native state to the A-state leads to a very striking reshuffling of the H-bond network in ubiquitin, which can be followed in detail by the $^{h3}J_{NC'}$ scalar correlations between H-bond donor and acceptor amino acids (Figure 1). These correlations clearly show that the H-bond patterns of the first antiparallel β-sheet and of the central α-helix are very similar under native state and A-state conditions. In contrast, the $^{h3}J_{NC'}$ correlations in the C-terminal part indicate numerous parallel and antiparallel β-sheet H-bonds in the native state, which switch to α-helical H-bonds in the A-state.

Figure 2A shows the size of the measured $^{h3}J_{NC'}$ couplings in the native state and A-state as a function of donor residue number. The change to the A-state increases the total number of detected backbone H-bonds (39 versus 32 in the native state), which have, however, weaker and more uniform $^{h3}J_{NC'}$ values. This trend is reflected in the average $|^{h3}J_{NC'}|$ value and its standard deviation, which are both smaller in the A-state (0.27 ± 0.10 Hz) than in the native state (0.50 ± 0.17 Hz). Neglecting angular dependencies and assuming a fixed geometry, smaller $|^{h3}J_{NC'}|$ values correspond to longer donor−acceptor distances (*18*, *22*). For the transition from the native state to the A-state, such an average lengthening of H-bonds is expected since a much larger fraction of H-bonds is α-helical in the A-state, and H-bonds are on average 0.1 Å longer in α-helices than in β-sheets (*30*). However, even within the conserved secondary structure elements ($\beta1$, $\beta2$, α), a clear reduction of the $^{h3}J_{NC'}$ values can be observed for many H-bonds (Figure 2A).

We attribute the reduced coupling size in the conserved structural elements to increased internal motions of the A-state. Since only single resonances are observed in the A-state, the internal motions are fast on the chemical shift time scale, i.e., faster than milliseconds. In fact, the reduced generalized order parameter extracted from ^{15}N-relaxation data by Brutscher and co-workers (*12*) indicates that the amplitudes of the pico- to nanosecond internal motions are larger than in the native state. However, the experimentally

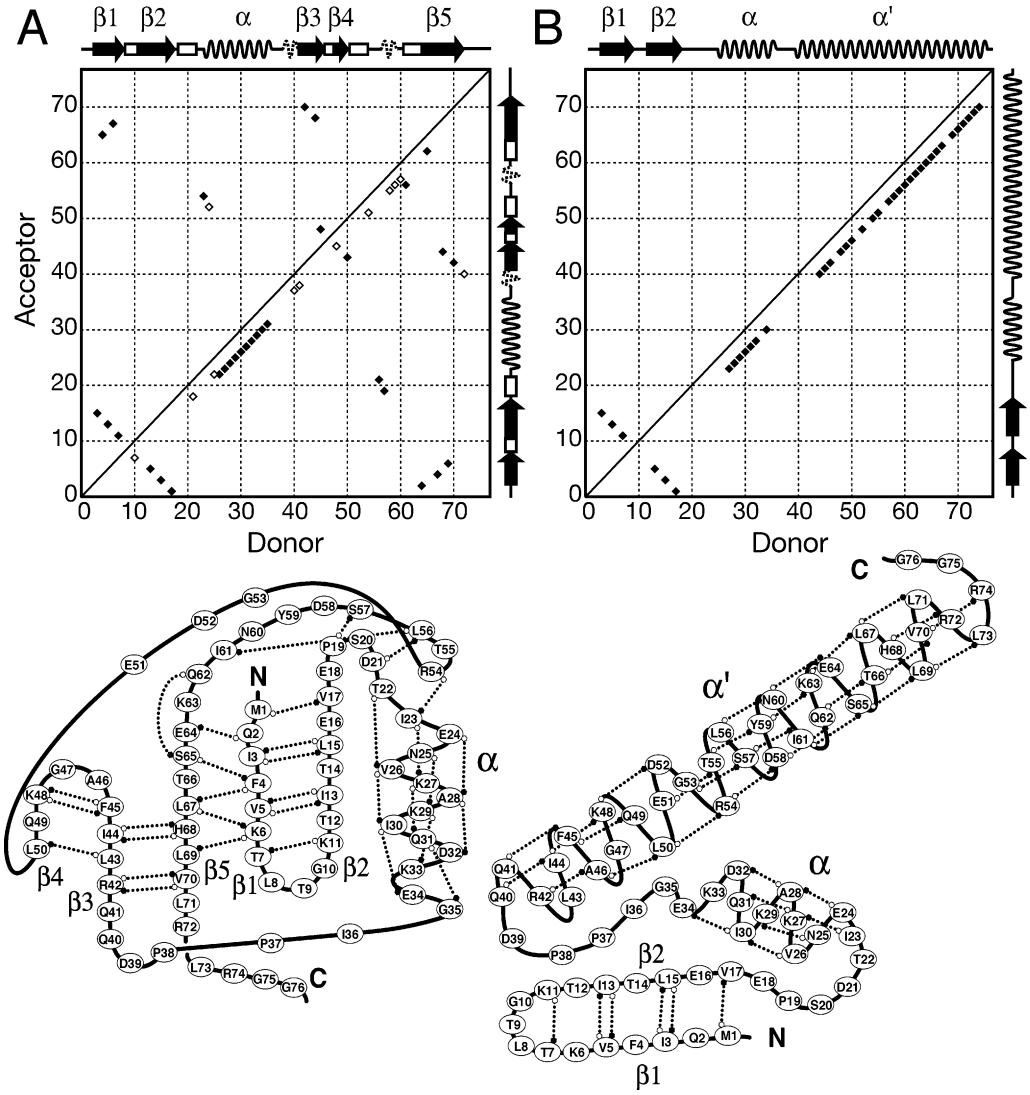

FIGURE 1: Hydrogen bond topologies as derived by detected $^{h3}J_{NC'}$ H-bond correlations for ubiquitin in the native state (A) and in the A-state (B). Top: two-dimensional maps representing the detected $^{h3}J_{NC'}$ scalar correlations (filled diamonds). Secondary structure elements are indicated as filled arrows for β-strands, solid wavy lines for α-helices, dashed wavy lines for 3_{10}-helices, and open boxes for β-turns. For the native state (A) open diamonds represent H-bonds, which were not detected by $^{h3}J_{NC'}$ correlations but which are present in the ubiquitin crystal structure (1UBQ) (*47*) with d_{OH} <2.5 Å and NH···O angles >120°. Bottom: H-bond topology diagrams derived for the two states based on detected $^{h3}J_{NC'}$ correlations. The H-bonds are depicted by a dotted line between the amide proton donors (filled hexagons) and the oxygen acceptors (open hexagons).

observed H-bond couplings could also be affected by motions, which are slower than the time scale of ^{15}N-relaxation experiments, because they represent time averages up to a time that is determined by the inverse of the coupling constants and the total time used for magnetization transfer, i.e., about 0.1−1 s. As their size depends exponentially on the H-bond distance (*21*, *22*) as well as on a number of H-bond angles (*21*, *23*, *24*), the time average of H-bond couplings corresponds to an average over these multivariate geometric dependencies. However, for larger amplitude motions the strong exponential distance dependence is expected to play a dominant role. Thus to a first approximation, the decrease in H-bond coupling size could be interpreted as an increase of the motional average of the H-bond length.

To compare the behavior of H-bonds in more detail, we describe in the following the changes in $^{h3}J_{NC'}$ values between both states separately for the different secondary structure elements.

Hairpin β1/β2. Strands β1 and β2 of native ubiquitin are connected by a "5-residue turn" (T7−K11) to form a twisted β-hairpin structure consisting of residues M1 to V17 (Figure 1). Apparently this structure forms independently from the rest of the protein (*16*), and it has been suggested that its formation constitutes an early event in ubiquitin's folding pathway (*31*, *32*). The conservation of this part of the secondary structure in the A-state is already evident from the deviations of the $^{13}C^{\alpha}$ and $^{13}C'$ chemical shifts from their random coil values (*12*). Panels B and C of Figure 2 show these secondary shifts for the $^{13}C^{\alpha}$ nuclei of the A-state and native state in comparison with the $^{h3}J_{NC'}$ data in Figure 2A. Negative values of the $^{13}C^{\alpha}$ secondary shifts, corresponding to a β-sheet conformation (*33*, *34*), are found for residues Q2−T7 and I13−E18 in both the native state and A-state. However, in the A-state, the secondary shifts have reduced absolute values. A similar observation was made for the $^{13}C^{\beta}$ secondary shifts in this β-sheet region (data not shown) where stronger positive values are found in the native state than in

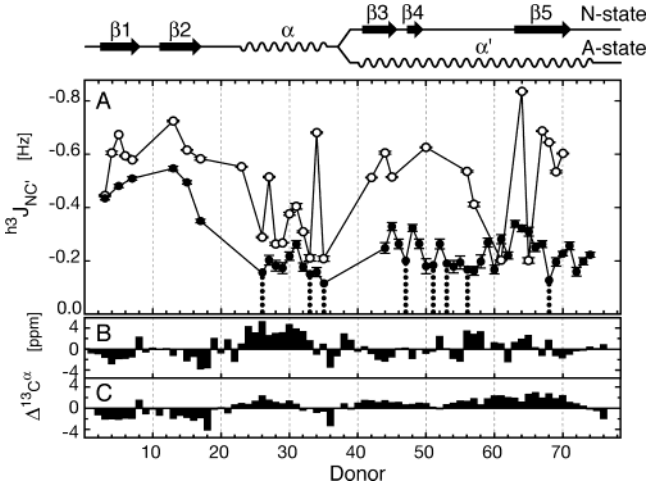

FIGURE 2: Comparison of $^{h3}J_{NC'}$ coupling constants and $^{13}C^{\alpha}$ secondary shifts in ubiquitin's native state and A-state. (A) Experimental $^{h3}J_{NC'}$ coupling constants versus donor residues in the native state (open circles) and in the partially folded A-state (filled circles). Error bars correspond to rms deviations of at least two independent experiments. In the A-state, filled circles connected to dotted lines indicate upper limits for $|^{h3}J_{NC'}|$ derived from the signal to noise ratio of the reference spectrum in cases where no H-bond cross-peaks could be detected (*17*). Secondary structure elements are indicated at the top for the native state and the A-state. $^{13}C^{\alpha}$ secondary shifts are indicated in (B) for the native state and in (C) for the A-state.

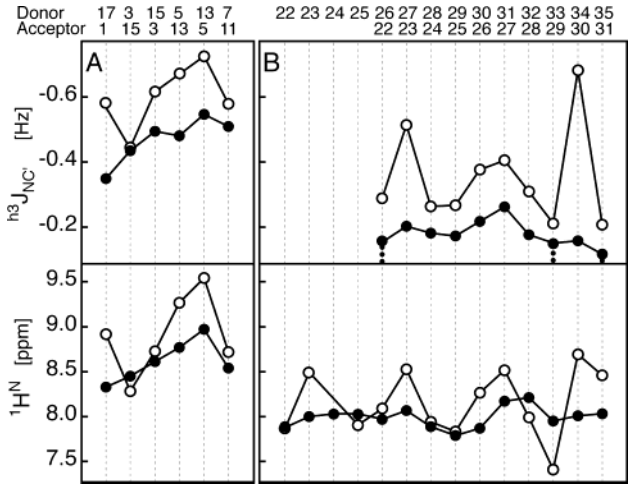

FIGURE 3: Comparison of $^{h3}J_{NC'}$ constants and $^{1}H^{N}$ chemical shifts in the conserved secondary structure elements of ubiquitin's native state (open circles) and A-state (filled circles). Data are arranged according to the secondary structure topology. (A) Hairpin $\beta1/\beta2$. (B) α-Helix α. Filled circles connected to dotted lines indicate upper limits for $|^{h3}J_{NC'}|$ in cases where no H-bond cross-peaks could be detected (see Figure 2).

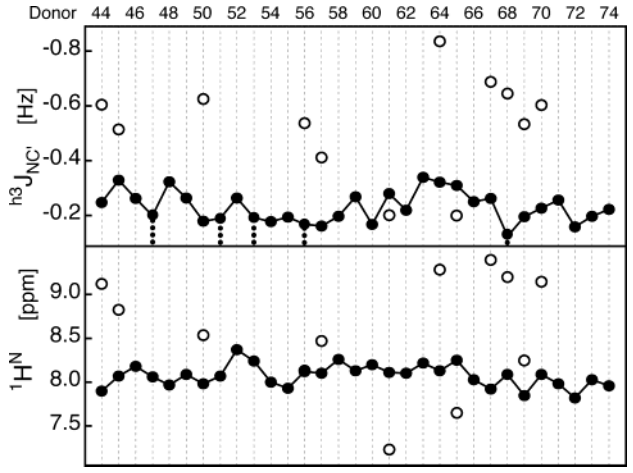

FIGURE 4: Comparison of $^{h3}J_{NC'}$ constants and $^{1}H^{N}$ chemical shifts in the nonconserved part of ubiquitin's secondary structure in the native state (open circles) and A-state (filled circles). Filled circles connected to dotted lines indicate upper limits for $|^{h3}J_{NC'}|$ in cases where no H-bond cross-peaks could be detected (see Figure 2).

the A-state. The reduction of the $^{13}C^{\alpha}$ secondary shifts has been interpreted previously as the result of the higher degree of internal dynamics of the A-state (*12*). The effect is also apparent in the average absolute size of the $^{h3}J_{NC'}$ scalar couplings (Figures 2A and 3A), which drops from a value of 0.63 ± 0.07 Hz ($N = 5$) in the native state to 0.48 ± 0.07 Hz ($N = 5$) in the A-state (omitting H-bond I3→L15, which has a particular behavior; see below). If interpreted as an H-bond length change (*25*), the ∼24% decrease in the couplings corresponds to an average lengthening ($\Delta r/\text{Å} = -1/4 \Delta^{h3}J_{NC'}/^{h3}J_{NC'}$) of about 0.07 Å. A strong correlation has been found between the $^{h3}J_{NC'}$ couplings and the $^{1}H^{N}$ chemical shifts (*18*, *25*), where large absolute-size $^{h3}J_{NC'}$ couplings correspond to strong $^{1}H^{N}$ downfield shifts, which are well-established indicators of short H-bond distances (*35*). This correlation is also evident from a comparison of $^{h3}J_{NC'}$ couplings and $^{1}H^{N}$ chemical shifts of H-bonding amino acids in the native state and A-state of ubiquitin (Figures 3 and 4). For the $\beta1/\beta2$ hairpin (Figure 3A), the reduction in the size of the $^{h3}J_{NC'}$ couplings corresponds to an average decrease in the amide proton chemical shift of about 0.4 ppm.

A particular behavior is found for the H-bond I3→L15 in the $\beta1/\beta2$ hairpin (Figure 3A). Whereas on average the H-bond strengths decrease considerably within this hairpin under A-state conditions, the NMR parameters for this H-bond remain virtually unchanged. The $^{h3}J_{NC'}$ value for this H-bond drops only slightly from −0.45 to −0.44 Hz, and the $^{1}H^{N}$ chemical shift shows even a slight increase. In a previous study on the temperature dependence of the H-bond properties of native ubiquitin (*25*), this H-bond also showed a very particular behavior: despite a strong temperature-induced decrease in the strength of the H-bond couplings and $^{1}H^{N}$ chemical shifts for residues in its direct vicinity, i.e., E64, M1, Q2, L15, and V17, the strength of the $^{h3}J_{N3C'15}$ coupling and the V3 $^{1}H^{N}$ chemical shift increased with increasing temperature from 5 to 65 °C. In native ubiquitin, the particularly strong H-bond E64→Q2 connects to the Q2/I3 amide group and coincides with a twist of the backbone conformation around residue I3 (Figure 1A). Apparently, the E64/Q2 contact exerts strain on residue I3, such that the latter is pulled away from its H-bond partner V15 toward residue E64. This is evidenced by a reduction of the $^{h3}J_{N3C'15}$ coupling as well as of the V3 $^{1}H^{N}$ chemical shift in the native state (Figure 3A). At higher temperatures, the $^{h3}J_{N64C'2}$ coupling shows a particularly strong decrease, consistent with a pronounced weakening of the E64/Q2 contact (*25*). This reduces the strain on residue I3 such that it can move closer toward V15. As a consequence, the $^{h3}J_{N3C'15}$ coupling as well as the V3 $^{1}H^{N}$ chemical shift increases slightly and becomes more equal to the neighboring H-bonded residues.

The behavior of the $^{h3}J_{NC'}$ couplings and $^{1}H^{N}$ chemical shifts within the $\beta1/\beta2$ hairpin of the A-state provides strong additional evidence for this mechanism. In the A-state, the E64→Q2 H-bond is absent, and the E64/Q2 contact cannot

distort the backbone conformation around residue I3. This leads to uniform $^{h3}J_{NC'}$ constants and $^{1}H^{N}$ chemical shifts across the entire β-sheet with no exceptional values for the I3→V15 H-bond (Figure 3A). On average, however, the $^{h3}J_{NC'}$ constants and $^{1}H^{N}$ chemical shifts are reduced relative to the native state because of the destabilizing environment of the acidic methanol/water phase. Thus, the behavior of the $\beta1/\beta2$ H-bonds in the A-state seems very similar to the onset of thermal unfolding in the native state. This onset is characterized by a global weakening of H-bond coupling constants and starts specifically by the destabilization of the E64→Q2 connection for temperatures above 60 °C (*25*).

The Central α*-Helix.* The $^{h3}J_{NC'}$ connectivities of the A-state (Figure 1A) show that all amide groups of residues I23 to E34 are bonded in $H^{N}(i)\rightarrow O(i-4)$ H-bonds. This confirms that the native central α-helix (residues T22 to G35) is largely conserved. The positive $^{13}C^{\alpha}$ secondary shifts are consistent with the helical structure of this region in the native state (Figure 2B) and A-state (Figure 2C). However, similar to hairpin $\beta1/\beta2$, the strongly reduced absolute size of the secondary shifts in the A-state indicates enhanced flexibility. Likewise, this effect is also visible in the reduction of the H-bond couplings (Figure 3B) with average $|^{h3}J_{NC'}|$ values of 0.35 ± 0.15 Hz ($N = 10$) in the native state but 0.20 ± 0.04 Hz ($N = 7$) in the A-state. Assuming again linear H-bond geometries, such a decrease corresponds to an average increase of donor−acceptor distances of about 0.11 Å in helix α *o*f the A-state.

A closer inspection of individual $^{h3}J_{NC'}$ scalar couplings and amide proton chemical shifts (Figure 3B) shows that the behavior of the H-bonds within the α-helix is by no means uniform. In native ubiquitin, very strong couplings (−0.4 to −0.7 Hz), associated with strong proton downfield shifts, are found for H-bonds K27→I23, I30→V26, Q31→K27, and E34→I30. These H-bonds are located on the face of the α-helix that is directed toward the hydrophobic core. Respectively, weaker couplings (−0.2 to −0.3 Hz) and more upfield proton chemical shifts are observed for H-bonds located at the exterior, water-exposed face of the helix. This leads to a pronounced periodicity of the $^{1}H^{N}$ chemical shifts, which is often found for amphipathic helices (*36*, *37*). On the basis of numerous observations of bent helices in crystal structures (*38*, *39*), it had been suggested that such periodicities are caused by different H-bond lengths on opposite helix sides, although an experimental proof from NMR data was missing (*36*). Clearly, ubiquitin's α-helix is amphipathic with hydrophobic residues (I23, V26, I30) at the interior and hydrophilic residues (E24, K29, K33) at the exterior side. From the observed periodicity in $^{h3}J_{NC'}$ values and $^{1}H^{N}$ chemical shifts, we concluded previously that indeed the H-bonds are shorter on the interior side and that ubiquitin's α-helix is bent around the hydrophobic core by about 9° (*25*).

In strong contrast to the native state, no such large periodicities in $^{h3}J_{NC'}$ couplings and $^{1}H^{N}$ chemical shifts are observed in the A-state. This is the consequence of a strong reduction in $^{h3}J_{NC'}$ size for the strong H-bonds K27→I23 and E34→I30 of the native state ($\Delta^{h3}J_{NC'} = 0.31$ and 0.52 Hz, respectively) and of much weaker reductions of about 0.1 Hz for the weaker H-bonds. As a result, all $^{h3}J_{NC'}$ couplings of this α-helix fall into a narrow range, −0.16 to −0.26 Hz, in the A-state. Similar changes are found for the $^{1}H^{N}$ chemical shifts, where the maximal variation around the average drops from ±0.74 ppm in the native state to ±0.22 ppm in the A-state. Thus both $^{h3}J_{NC'}$ couplings and $^{1}H^{N}$ chemical shifts indicate that the H-bonds have comparable strengths across the entire helix and that the bend of the helix in the native state is largely released in the A-state. Apparently, the replacement of the strongly asymmetric hydrophobic/hydrophilic contacts on both sides of the helix by a homogeneous methanol/water environment leads to a more straight and symmetric structure of the helix.

The Elongated C-Terminal Helical Segment. The $^{h3}J_{NC'}$ correlations in the C-terminal part of ubiquitin's A-state structure (Figure 1) yield a large number of H-bond connectivities. These clearly confirm the helical nature of this segment as it was derived from CD (*6*, *7*), heteronuclear chemical shift, and short-range NOE data (*11*, *12*) but had not been detected in the early homonuclear NMR work (*8*, *10*). Despite the high internal flexibility of the long C-terminal helix with a nanosecond order parameter S^2 of about 0.6 (*12*), almost all amide groups for residues I44 to R74 yield observable $H^{N}(i)\rightarrow O(i-4)$ $^{h3}J_{NC'}$ correlations (Figures 1 and 4). Thus the $^{h3}J_{NC'}$ data unambiguously establish that the helix has α-helical periodicity, a fact which could not be derived earlier due to the absence of indicative, medium-range $H^{\alpha}{}_{i}-H^{N}{}_{i+3}/H^{N}{}_{i+4}$ NOE contacts (*12*).

The transition from the native β-sheet structure of the C-terminal part of ubiquitin to the extended α-helical structure in the A-state causes a strong reduction in the average size and dispersion of $^{h3}J_{NC'}$ values (Figure 4). However, the total number of detected backbone H-bonds involving a donor or an acceptor group in the C-terminal part increases from 16 to 26 (Figure 1). This is consistent with the fact that helical conformations usually have a larger number of intramolecular backbone H-bonds than β-sheet structures. The behavior of the $^{h3}J_{NC'}$ values is mirrored in the $^{1}H^{N}$ chemical shifts, which show a similar reduction in size and dispersion. Both quantities are rather uniform across the entire C-terminal helix with average values of -0.24 ± 0.05 Hz for $^{h3}J_{NC'}$ and 8.07 ± 0.13 ppm that are very similar to the values in the central α-helix (Figure 3B).

A certain variation within this uniform segment is evident for donor residues G53 to D58 (Figure 4). In this region, the $|^{h3}J_{NC'}|$ values are below 0.2 Hz, and the $^{13}C^{\alpha}$ and $^{13}C'$ secondary chemical shifts for acceptor residues around D52 are reduced (Figure 2C and ref *12*). In addition, $H^{N}{}_{i}-H^{N}{}_{i-3}$ NOEs for $i =$ D52 and G53 are observable in the long-range ^{15}N-edited NOESY (data not shown). Only minor variations were found for this region in the ^{15}N-relaxation data (*12*). It is therefore possible that this part of the helix is either statically distorted or that a dynamic destabilization occurs on a time scale, e.g., submicrosecond, which does not strongly affect the ^{15}N-relaxation measurements.

DISCUSSION

The hydrogen bond network of the partially folded A-state of ubiquitin has been compared to the native state by a detailed analysis of the trans hydrogen bond $^{h3}J_{NC'}$ scalar couplings and $^{1}H^{N}$ chemical shifts. Despite the large flexibility of the A-state, most of the $^{h3}J_{NC'}$ couplings could be measured with high precision and reproducibility. In the A-state, the average size of $^{h3}J_{NC'}$ couplings is reduced, but a larger number of backbone H-bonds can be detected due

to the higher α-helical content. The data clearly show the conservation of hairpin $\beta1/\beta2$ and the central α-helix, whereas the C-terminal part is transformed into a long, purely α-helical segment. The reduced size of $^{h3}J_{NC'}$ couplings in the conserved parts of the ubiquitin structure coincides with the decrease of the $^{13}C^{\alpha}$ and $^{13}C'$ secondary shifts and is attributed to motional averaging.

To our knowledge, partially folded states have only been characterized by $^{h3}J_{NC'}$ couplings for the case of the TFE-induced folding of the small 22 amino acid S-peptide (*40*). In this case, the fast exchange between unfolded and folded conformations together with the strong dependence on the H-bond N−O distance (*18*, *21*, *22*) justifies the approximation that $^{h3}J_{NC'}$ values are proportional to the population of closed H-bonds. This was verified by the close correlation between $^{h3}J_{NC'}$-derived populations and predictions of the Zimm−Bragg (*41*) and Lifson−Roig (*42*, *43*) theories of the coil to α-helix transition. In the case of A-state ubiquitin, this approximation seems more problematic, because the equilibrium is closer to the folded state such that small variations in the average N−O distance play a larger role. Neglecting this complication, one could also assume a simple two-state model of closed and open H-bonds for ubiquitin. In this picture, the reduction in $^{h3}J_{NC'}$ of the A-state would then correspond to a reduction of the probability to find individual H-bonds in a closed state, rather than assuming that the average H-bond length is increased.

A large body of literature exists on the characterization of partially folded states by hydrogen-exchange (HX) experiments (*44*, *45*). However, no close correlation between HX rates and H-bond coupling constants was found in an extensive study on the temperature dependence of H-bond parameters in ubiquitin (*25*). This absence of correlation is not really surprising since both parameters report on different molecular properties. In the usual exchange models, it is assumed that HX occurs from an open H-bond but that the exchange can be hindered by the surrounding molecular structure (*46*). Thus the exchange rates report on the combined effect of H-bond opening and solvent accessibility. In contrast, the H-bond scalar couplings report the average of the H-bond geometry. For the current study, HX rates were also determined for A-state ubiquitin. However, no noteworthy features could be detected besides that exchange is stronger in the loop regions than in the α-helical and β-sheet parts of the structure (data not shown).

The observed changes in $^{h3}J_{NC'}$ couplings in all parts of the A-state structure strongly correlate to changes in $^{1}H^{N}$ chemical shifts. In general, the size of the $^{h3}J_{NC'}$ couplings and $^{1}H^{N}$ chemical shifts is much more homogeneous across the different secondary structure elements in the A-state than in the native state. Strong heterogeneities in the size of these parameters had been observed previously in native state of ubiquitin for residue I3 within hairpin $\beta1/\beta2$ and for the interior side of the central α-helix (*25*). These anomalities had been interpreted as a distortion around residue I3 due to a very strong I64/Q2 contact and as a bend of the amphipathic central helix around ubiquitin's hydrophobic core. No such heterogeneities are observed in the $\beta1/\beta2$ hairpin and the central α-helix of the A-state. Thus the heterogeneities in the native state are caused by tertiary interactions to other parts of the protein, and a replacement of these contacts by the homogeneous environment of the 40%/60% water/methanol mixture leads to very uniform H-bonds and regular secondary structure conformations. In many aspects, this state is similar to the onset of thermal denaturation observed at temperatures above 60 °C (*25*). In summary, this combined analysis of H-bond correlations and chemical shifts provides a detailed and rational picture of the dynamic interactions that distinguish a partially folded from a completely folded protein state.

ACKNOWLEDGMENT

We thank Bernhard Brutscher and Rafael Brueschweiler for very valuable discussions and Marco Rogowski for expert protein preparation.

REFERENCES

1. Ohgushi, M., and Wada, A. (1983) "Molten-globule state": a compact form of globular proteins with mobile side-chains, *FEBS Lett. 164*, 21−24.
2. Kuwajima, K. (1989) The molten globule state as a clue for understanding the folding and cooperativity of globular-protein structure, *Proteins 6*, 87−103.
3. Alexandrescu, A. T., and Shortle, D. (1994) Backbone dynamics of a highly disordered 131 residue fragment of staphylococcal nuclease, *J. Mol. Biol. 242*, 527−546.
4. Ptitsyn, O. B. (1995) Molten globule and protein folding, *Adv. Protein Chem. 47*, 83−229.
5. Ptitsyn, O. B. (1995) Structures of folding intermediates, *Curr. Opin. Struct. Biol. 5*, 74−78.
6. Wilkinson, K. D., and Mayer, A. N. (1986) Alcohol-induced conformational changes of ubiquitin, *Arch. Biochem. Biophys. 250*, 390−399.
7. Cox, J. P., Evans, P. A., Packman, L. C., Williams, D. H., and Woolfson, D. N. (1993) Dissecting the structure of a partially folded protein. Circular dichroism and nuclear magnetic resonance studies of peptides from ubiquitin, *J. Mol. Biol. 234*, 483−492.
8. Pan, Y., and Briggs, M. S. (1992) Hydrogen exchange in native and alcohol forms of ubiquitin, *Biochemistry 31*, 11405−11412.
9. Briggs, M. S., and Roder, H. (1992) Early hydrogen-bonding events in the folding reaction of ubiquitin, *Proc. Natl. Acad. Sci. U.S.A. 89*, 2017−2021.
10. Harding, M. M., Williams, D. H., and Woolfson, D. N. (1991) Characterization of a partially denatured state of a protein by two-dimensional NMR: reduction of the hydrophobic interactions in ubiquitin, *Biochemistry 30*, 3120−3128.
11. Stockman, B. J., Euvrard, A., and Scahill, T. A. (1993) Heteronuclear three-dimensional NMR spectroscopy of a partially denatured protein: the A-state of human ubiquitin, *J. Biomol. NMR 3*, 285−296.
12. Brutscher, B., Bruschweiler, R., and Ernst, R. R. (1997) Backbone dynamics and structural characterization of the partially folded A state of ubiquitin by ^{1}H, ^{13}C, and ^{15}N nuclear magnetic resonance spectroscopy, *Biochemistry 36*, 13043−13053.
13. Jourdan, M., and Searle, M. S. (2001) Insights into the stability of native and partially folded states of ubiquitin: effects of cosolvents and denaturants on the thermodynamics of protein folding, *Biochemistry 40*, 10317−10325.
14. Alonso, D. O., and Daggett, V. (1995) Molecular dynamics simulations of protein unfolding and limited refolding: characterization of partially unfolded states of ubiquitin in 60% methanol and in water, *J. Mol. Biol. 247*, 501−520.
15. Prompers, J. J., Scheurer, C., and Bruschweiler, R. (2001) Characterization of NMR relaxation-active motions of a partially folded A-state analogue of ubiquitin, *J. Mol. Biol. 305*, 1085−1097.
16. Zerella, R., Evans, P. A., Ionides, J. M., Packman, L. C., Trotter, B. W., Mackay, J. P., and Williams, D. H. (1999) Autonomous folding of a peptide corresponding to the N-terminal beta-hairpin from ubiquitin, *Protein Sci. 8*, 1320−1331.
17. Grzesiek, S., Cordier, F., and Dingley, A. J. (2001) Scalar couplings across hydrogen bonds, *Methods Enzymol. 338*, 111−133.

18. Cordier, F., and Grzesiek, S. (1999) Direct observation of hydrogen bonds in proteins by interresidue $^{3h}J_{NC'}$ scalar couplings, *J. Am. Chem. Soc. 121*, 1601−1602.
19. Cornilescu, G., Hu, J. S., and Bax, A. (1999) Identification of the hydrogen bonding network in a protein by scalar couplings, *J. Am. Chem. Soc. 121*, 2949−2950.
20. Barfield, M., Dingley, A. J., Feigon, J., and Grzesiek, S. (2001) A DFT study of the interresidue dependencies of scalar J-coupling and magnetic shielding in the hydrogen-bonding regions of a DNA triplex, *J. Am. Chem. Soc. 123*, 4014−4022.
21. Barfield, M. (2002) Structural dependencies of interresidue scalar coupling (h3)J(NC′) and donor (1)H chemical shifts in the hydrogen bonding regions of proteins, *J. Am. Chem. Soc. 124*, 4158−4168.
22. Cornilescu, G., Ramirez, B. E., Frank, M. K., Clore, G. M., Gronenborn, A. M., and Bax, A. (1999) Correlation between $^{3h}J_{NC'}$ and hydrogen bond length in proteins, *J. Am. Chem. Soc. 121*, 6275−6279.
23. Scheurer, C., and Brüschweiler, R. (1999) Quantum-chemical characterization of nuclear spin−spin couplings across hydrogen bonds, *J. Am. Chem. Soc. 121*, 8661−8662.
24. Bagno, A. (2000) Quantum chemical modeling of through-hydrogen bond spin−spin coupling in amides and ubiquitin, *Chem. Eur. J. 6*, 2925−2930.
25. Cordier, F., and Grzesiek, S. (2002) Temperature-dependence properties as studied by of protein hydrogen bond high-resolution NMR, *J. Mol. Biol. 317*, 739−752.
26. Sass, J., Cordier, F., Hoffmann, A., Cousin, A., Omichinski, J. G., Lowen, H., and Grzesiek, S. (1999) Purple membrane induced alignment of biological macromolecules in the magnetic field, *J. Am. Chem. Soc. 121*, 2047−2055.
27. Piotto, M., Saudek, V., and Sklenar, V. (1992) Gradient-tailored excitation for single-quantum NMR spectroscopy of aqueous solutions, *J. Biomol. NMR 2*, 661−665.
28. Grzesiek, S., and Bax, A. (1993) The importance of not saturating H_2O in protein NMR−Application to sensitivity enhancement and NOE measurements, *J. Am. Chem. Soc. 115*, 12593−12594.
29. Wang, Y. X., Jacob, J., Cordier, F., Wingfield, P., Stahl, S. J., Lee-Huang, S., Torchia, D., Grzesiek, S., and Bax, A. (1999) Measurement of $^{3h}J_{NC'}$ connectivities across hydrogen bonds in a 30 kDa protein, *J. Biomol. NMR 14*, 181−184.
30. Baker, E. N., and Hubbard, R. E. (1984) Hydrogen bonding in globular proteins, *Prog. Biophys. Mol. Biol. 44*, 97−179.
31. Khorasanizadeh, S., Peters, I. D., and Roder, H. (1996) Evidence for a three-state model of protein folding from kinetic analysis of ubiquitin variants with altered core residues, *Nat. Struct. Biol. 3*, 193−205.
32. Zerella, R., Chen, P. Y., Evans, P. A., Raine, A., and Williams, D. H. (2000) Structural characterization of a mutant peptide derived from ubiquitin: implications for protein folding, *Protein Sci. 9*, 2142−2150.
33. Spera, S., and Bax, A. (1991) Empirical correlation between protein backbone conformation and C^{α} and C^{β} ^{13}C nuclear magnetic resonance chemical shifts, *J. Am. Chem. Soc. 113*, 5490−5492.
34. Wishart, D. S., and Sykes, B. D. (1994) The ^{13}C chemical-shift index: a simple method for the identification of protein secondary structure using ^{13}C chemical-shift data, *J. Biomol. NMR 4*, 171−180.
35. Wagner, G., Pardi, A., and Wuethrich, K. (1983) Hydrogen bond length and proton NMR chemical shifts in proteins, *J. Am. Chem. Soc. 105*, 5948−5949.
36. Kuntz, I. D., Kosen, P. A., and Craig, E. C. (1991) Amide chemical shifts in many helices in peptides and proteins are periodic, *J. Am. Chem. Soc. 113*, 1406−1408.
37. Zhou, N. E., Zhu, B.-Y., Sykes, B. D., and Hodges, R. S. (1992) Relationship between amide proton chemical shifts and hydrogen bonding in amphipathic α-helical peptides, *J. Am. Chem. Soc. 114*, 4320−4326.
38. Blundell, T., Barlow, D., Borkakoti, N., and Thornton, J. (1983) Solvent-induced distortions and the curvature of alpha-helices, *Nature 306*, 281−283.
39. Chakrabarti, P., Bernard, M., and Rees, D. C. (1986) Peptide-bond distortions and the curvature of alpha-helices, *Biopolymers 25*, 1087−1093.
40. Jaravine, V. A., Alexandrescu, A. T., and Grzesiek, S. (2001) Observation of the closing of individual hydrogen bonds during TFE- induced helix formation in a peptide, *Protein Sci. 10*, 943−950.
41. Zimm, B. H., and Bragg, J. K. (1959) Theory of the phase transition between helix and random coil in polypeptide chains, *J. Chem. Phys. 31*, 526−535.
42. Lifson, S., and Roig, A. (1961) Theory of helix-coil transition in polypeptides, *J. Chem. Phys. 34*, 1963−1974.
43. Qian, H., and Schellman, J. A. (1992) Helix-coil theories: A comparative study for finite length polypeptides, *J. Phys. Chem. 96*, 3987−3994.
44. Baldwin, R. L. (1993) Pulsed H/D-exchange studies of folding intermediates, *Curr. Opin. Struct. Biol. 3*, 84−91.
45. Englander, S. W. (2000) Protein folding intermediates and pathways studied by hydrogen exchange, *Annu. Rev. Biophys. Biomol. Struct. 29*, 213−238.
46. Englander, S. W. (1996) Hydrogen Exchange & Macromolecular Dynamics, in *Encyclopedia of Nuclear Magnetic Resonance* (Grant, D. M., and Harris, R. K., Eds.) Vol. 4, pp 2415−2420, John Wiley, New York.
47. Vijay-Kumar, S., Bugg, C. E., and Cook, W. J. (1987) Structure of ubiquitin refined at 1.8 Å resolution, *J. Mol. Biol. 194*, 531−544.

BI049314F